Proceedings of the 20th Annual International Conference of the IEEE Engineering in Medicine and Biology Society, Vol. 20, No 2, 1998

3D ELASTIC MULTIMODALITY IMAGE REGISTRATION THROUGH A GENETIC ALGORITHM

Jean-Michel Rouet, Jean-José Jacq and Christian Roux

Département Image et Traitement de l'Information
Laboratoire de Traitement de l'Information Médicale
ENST Bretagne, Technopôle Brest-Iroise
BP 832 - 29285 Brest Cédex - FRANCE
E-mail: JM.Rouet@enst-bretagne.fr

Abstract

This paper deals with the matching of two numerical surfaces through an elastic 3D transformation. The global search of the optimal transformation is performed using a new genetic algorithm while taking into account the local curvature on the surfaces. Then, we operate a local optimization using the information contained in the final genetic population.

1 Introduction

In medical imaging, registration is a common prerequisite to the effective use of multiple sources of image data. The existence of slight distortions inherent to each modality prevents the user from finding easily a good rigid matching. As the number of parameters involved in such a registration process becomes quite high, complex matching algorithms are required.

Besides their diversity, almost all the registration techniques [1] [2] [3] share a common aspect: the evaluation of a distance (or an error) that measures how far two different images are. Once the measurement is chosen, the next step is to find an optimization algorithm which looks for the transformation (within a set of allowed geometric transformations) that minimizes this distance (or error). The new method we have developped is based on a particular encoding of an elastic 3D transformation coupled with an optimization through a genetic algorithm. This solving approach seems to become more and more used because of its efficiency [4] [5] [6] [7] [8] [9].

2 Description of the work

The images we are dealing with are a head CT-scan volume composed of 92 slices (256x256 pixels), and a set of 65 slices (256x256) from an MRI exam of the same head. The actual size of the voxel differs from one modality to the other. We consider one to be the reference and the other one to be registered. For instance we choose as a reference the CT image and the result of the algorithm is a warped image of the MRI volume. Consequently, in order to achieve the warping, we are aiming at a function which transforms each point of the reference image to its estimated homologous in the 'to be registered' image. As stated above, the geometric transformation we are looking for is a 3D elastic one. We assume that a global transformation modeled by a trilinear warping is sufficient enough to represent noticeable global morphological variations between the two structures that we are matching. In the 3D case, such a transformation can be expressed by

$$\begin{cases} x_1 = \sum_{p=0}^{1}\sum_{q=0}^{1}\sum_{r=0}^{1} a_{p,q,r} x_0^p y_0^q z_0^r \\ y_1 = \sum_{p=0}^{1}\sum_{q=0}^{1}\sum_{r=0}^{1} b_{p,q,r} x_0^p y_0^q z_0^r \\ z_1 = \sum_{p=0}^{1}\sum_{q=0}^{1}\sum_{r=0}^{1} c_{p,q,r} x_0^p y_0^q z_0^r \end{cases} \quad (1)$$

where $(x_1, y_1, z_1) = T(x_0, y_0, z_0)$ denotes the transformed positions of site (x_0, y_0, z_0) of the reference image. The corresponding search space has $L = 24$ dimensions.

In order to facilitate the matching process we do not work directly on the raw images, but we consider pertinent information issued from a preprocessing step. For our head images, the easier extractable common feature is the boundary surface which separates the air from the skin thus our matching process is resumed to the matching of two numerical surfaces. These surfaces are computed using morphological mathematic tools; the segmentation algorithm is beyond the scope of this paper and will not be described here. Eventually, the evaluation of the goodness of fit of our two surfaces can be achieved by the use of a distance map [10] (a 3D-image derived from a numerical surface where the value of each voxel represents an approximation of the Euclidian distance between this voxel and the numerical surface).

0-7803-5164-9/98/$10.00 © 1998 IEEE

3 Optimization process through a genetic algorithm

The transformation described by (1) has 24 parameters. These parameters allow to calculate the transformed location of every site from the reference image to the registered image. Besides, the knowledge of the transformed position of exactly 8 different sites is just enough to reverse compute the corresponding 24 parameters[1]. Considering the two numerical surfaces as two points sets, the matching algorithm just has to find 8 points from each set that correspond each other. Since the typical size of the sets varies between 30000 and 60000 points, the number of possible associations is huge, hence the search space is very large. That is why we are using a genetic algorithm to explore that search space. Each chromosome (a tentative solution) of the genetic population represents a set of 8 couples of points, as shown by figure 1.

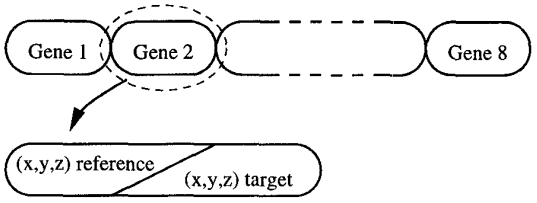

Figure 1: encoding of a chromosome

Basically, a genetic algorithm is a global stochastic optimization procedure which uses the properties of the evolution of natural systems. The algorithm acts on an iterative way by allowing parallel evolution in a population of N individuals which represents a point of the search space. The appropriateness of each individuals is measured by a fitness function. The basic principle is to let the population evolve by recombining on a random way chromosomes two by two (operation known as *cross-over*), and by modifying randomly the features of the chromosome (it is the *mutation*). Then, at each step, the selection of the N individuals is carried out by cloning the best individuals, dropping the worst and keeping the others. Successive application of these operators let evolve the population with a constant number of individuals across the generations.

A stochastic computation of the performance of each chromosome is used in order to speed up the optimization process. A fixed number n of randomly chosen sites on the reference surface are projected, using the chromosome's decoded parameters, onto the distance map. The mean error is then computed as the average of the observed distances. In order to have a function maximizing performance value, effective computation is done through the formula[2] (2)

$$\mathrm{perf}(T) = \frac{1}{n}\sum_{i=1}^{n} \varphi(d(T(p_i))), \text{ with } \varphi(x) = e^{-x^2/\sigma^2}, \quad (2)$$

and thus

$$0 \leqslant \mathrm{perf}(T) \leqslant 1, \quad (3)$$

where p_i represents the position of the ith randomly chosen point of the reference surface, $d(T(p_i))$ is the value read on the distance map at the transformed position of p_i by the T 3D elastic transformation. In the following experiments the smoothing coefficient σ is chosen the value 4mm.

In order to reduce a bit the search space, we are filtering the possible associations by two means:

- At first, we are calculating for each point of the two surfaces the value of local curvatures like the Gaussian curvature. Then, we classify the points with respect to the value of the curvature. This classification allows us to tolerate the association between points of the same class only. For instance, we do not want our algorithm to try to associate points with a positive curvature on an image with points with a negative curvature on the other image.

- The other way of reducing the size of the search space is to initiate the algorithm by a fast (and thus with a limited accuracy) rigid registration. A rigid registration consists in finding 3 rotation and 3 translation parameters and results in giving a global estimation of the mutual neighborhood of the surfaces associated with a confidence interval (derived from the calculated goodness of fit of the transformation). The information of the mutual neighborhood is used to obtain a first approximation of the actual distance between a point of one surface and the points of the other surface. Then, as shown in figure 2, we can constrain the association between points to the same neighborhood only (within the range of the confidence interval).

4 Stopping criterion

One of the problems while using a genetic algorithm is to decide when to stop the algorithm. The optimization process could be stopped when a certain goodness of fit has been reached or after a certain number of iterations has been performed. In fact, there is no way to check whether the right solution has been found or not. In the field of genetic algorithms the choice of termination is still

[1] This is only true when the 8 reference sites are distinct as for the 8 corresponding sites.

[2] Moreover, this formula includes matching abilities; this results in a better handling of the points from the reference image which do not have an homologous in the other image.

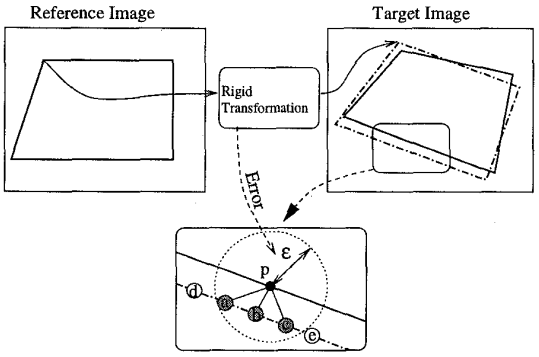

Figure 2: The possible association with the point p according to a certain rigid transformation whose error is ϵ are the points a, b and c. We assume that all the considered points belongs to the same curvature class.

an open problem. The approach we propose is to set two thresholds parameters controlling the stopping criterion. The first one is based on the goodness of fit. Given the equation (3), the maximum reachable value for the fitness function is 1; so if this value is reached, the optimization process can stop. The second threshold is an arbitrary one which stops the algorithm after a fixed number of iterations. It prevents the algorithm from running infinitely. Once the genetic algorithm optimization process is over, the solution to take into account can be chosen. The first method we can think of just considers taking the best individual among all the chromosomes of the population. This approach is suboptimal because it does not take advantage of all the information contained in the other individuals. The method we use consists in an adaptive filtering of the final population leading to a subset[3] whose global performance is better than the best individual performance. The performance of a group of chromosomes is computed by solving the over-determined system generated by the whole set of associations described by the individuals of the subset. We start from a one-member subset containing only the best individuals and we are looking iteratively if the adjunction of one new element in the subsset increases the performance. The process stops when any adjunction do not improve the performance.

5 Validating the results

Once the registration is performed we can focus on results validation. Various methods are possible like considering the raw performance only. This method only gives an idea of the goodness of fit but is not good enough to decide if the result is far from what we were waiting for or not. Moreover, the raw performance is a stochastic variable and its mean value only indicates the global

[3]containing at least the best individual of the final population.

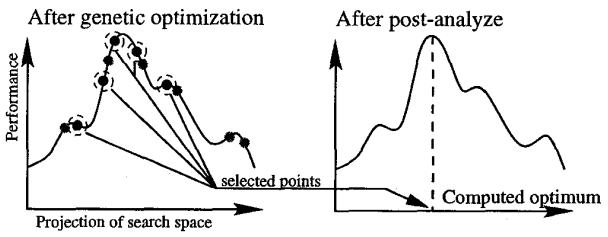

Figure 3: The post-analyze process consists in selecting chromosomes issued from the final genetic population whose group performance is better than each individual.

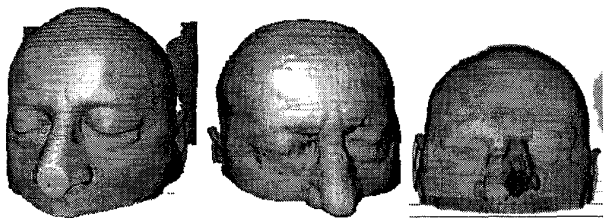

(a) CT (b) IRM (c) Initial misregistration

Figure 4: Initial images

adjustment. To estimate the actual goodness of fit, a raw performance is of no use without a visual validation. For that purpose we use a direct multi-volume rendering (DVR) tool [11] that enable fuzzy surface intersection rendering between the two numerical surfaces involved by the registration algorithm (see images 5(a), 5(b) and 5(c)).

(a) CT ∩ MRI (b) CT ∩ MRI (c) CT ∪ MRI

Figure 5: DVR validation

Moreover, depending on the sources of the images to register, we can validate the results by visualizing the interesting features of each modality at the same time. For instance, CT-scans give a good localization and definition of the bones while MRI images give good anatomical infor-

mation except for bones and rigid materials. If we extract – through some threshold – the regions corresponding to the bone material from the CT image we can superimpose it on the grey-scale MRI image (as figured out by images 6(a), 6(b) and 6(c)). Thus, we join the useful information of both modalities in one image.

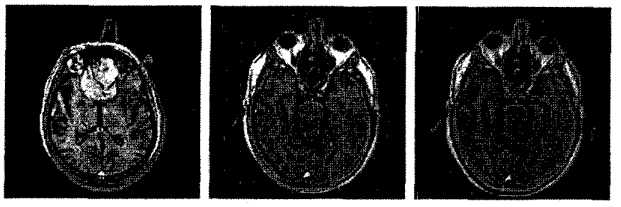

(a) before registration (b) rigid registration (c) elastic registration

Figure 6: Structural validation

The figures 4, 5 and 6 summarize the results. The CT scan reference image, and the MRI to be registered are shown in 4(a) and 4(b). The initial misalignement is shown in 4(c). We can then appreciate the renderings given by the DVR algorithm showing the intersection (figure 5(a) and 5(b)) and the union (figure 5(c)) between the two registered volumes. On the intersection images we remark only a hole at the right behind and at the full behind of the head wich denotes how well the two numerical surfaces are registered (when misaligned, the intersection is almost empty). Eventually the bone structure matching is shown for the unregisterd images (figure 6(a)), after rigid matching (figure 6(b)) and after elastic registration (figure 6(c)).

6 Conclusion

The work presented in this paper shows that 3D elastic multimodality registration gives interesting results. The robustness of the algorithm over the problem of local extrema is a big asset versus the other global optimization algorithms. The better the encoding scheme, the more efficient will be the genetic algorithm. The original encoding using information like local curvature we have investigated seems to be a good choice. Moreover, the use of a fast rigid registration step improves largely the performance of the algorithm by restraining the search space to only almost realistic association. For further work, we plan to evaluate the effective robustness of the algorithm on synthetic geometrical objects and to perform clinical validations of this approach.

Acknowledgments

We would like to thank Stéphane Lavallée from the "Technique de l'Imagerie, de la Modélisation et de la Cognition (TIMC) de Grenoble" laboratory for providing the MRI and CT scans.

References

[1] H. BARROW and al, "Parametric correspondance and chamfer matching : Two new techniques for image matching," in *Proceedings of the 5th International Joint Conference on Artificial Intelligence* (R. REDDY, ed.), (Cambridge), pp. 659–663, MA, August 1977.

[2] G. BORGEFORS, "Hierarchical chamfer matching: A parametric edge matching algorithm," *IEEE Transactions on Pattern Analysis and Machine Intelligence*, vol. 10, pp. 849–865, Nov. 1988.

[3] P. VAN DEN ELSEN, "Medical image matching – a review with classification," *IEEE EMBS Magazine*, pp. 26–39, March 1993.

[4] J. FITZPATRICK and J. GREFENSTETTE, "Genetic algorithms in noisy environments," *Machine Learning*, vol. 3, no. 2-3, pp. 101–120, 1988.

[5] J.-J. JACQ and C. ROUX, "Registration of 3-d images by genetic optimization," *Pattern Recognition Letters*, vol. 16, pp. 823–841, August 1995.

[6] L. H. STAIB and X. LEI, "Intermodality 3-d medical imaging registration with global search," in *IEEE Worksop on Biomedical Analysis*, pp. 225–234, 1994.

[7] BRUNSTRÖM and STODDART, "Genetic algorithms for free-form surface matching," in *ICPR'96*, March 1996.

[8] J.-M. ROUET, J.-J. JACQ, and C. ROUX, "Recalage 3d élastique de surfaces numériques par optimisation génétique," in *GRETSI'97*, vol. 2, (Grenoble), Septembre 1997.

[9] J.-J. JACQ and C. ROUX, "Automatic registration of 3d images using a simple genetic algorithm with a stochastic performance function," in *Proceeding of EMBS 93 – invitted paper, San diego*, pp. 90–91, October 1993.

[10] T. SAÏTO and J. TORIWAKI, "New algorithms for euclidian distance transformation of a n-dimensional digitized picture with applications," *Pattern Recognition*, vol. 27, pp. 66–88, July 1994.

[11] J.-J. JACQ and C. ROUX, "A direct multi-volume rendering method aiming at comparisons of 3-d images and models," *IEEE Trans. on Information Technology in Biomedecine*, vol. 1, pp. 30–43, Mar. 1997.